A Micromachined Silicon Sieve Electrode for Nerve Regeneration Applications

Tayfun Akin, *Student Member, IEEE,* Khalil Najafi, *Member, IEEE,* Richard H. Smoke, and Robert M. Bradley

***Abstract*—A micromachined silicon sieve electrode has been developed and fabricated to record from and stimulate axons/fibers of the peripheral nervous system by utilizing the nerve regeneration principle. The electrode consists of a 15-μm-thick silicon support rim, a 4-μm-thick diaphragm containing different size holes to allow nerve regeneration, thin-film iridium recording/stimulating sites, and an integrated silicon ribbon cable, all fabricated using boron etch-stop and silicon micromachining techniques. The thin diaphragm is patterned using reactive ion etching to obtain different size holes with diameters as small as 1 μm and center–center spacings as small as 10 μm. The holes are surrounded by 100–200 μm^2 anodized iridium oxide sites, which can be used for both recording and stimulation. These sites have impedances of less than 100 kΩ @ 1 kHz and charge delivery capacities in the 4–6 mC/cm^2 range. The fabrication process is single-sided, has high yield, requires only five masks, and is compatible with integrated multilead silicon ribbon cables. The electrodes were implanted between the cut ends of peripheral taste fibers of rats (glossopharyngeal nerve), and axons functionally regenerated through holes, responding to chemical, mechanical, and thermal stimuli.**

I. Introduction

RECORDINGS of neural activity in the central and peripheral nervous systems have been pivotal in understanding how the brain processes information to control all basic bodily functions. Recordings of neural signals from the central nervous system, either *in vivo* or *in vitro*, are accomplished using intra- and extracellular microelectrodes [1]–[3], whereas hook and cuff electrodes are mostly used to record from the peripheral nervous system. Some investigators have also used combinations of cuff electrodes and microelectrodes to interface with the peripheral nervous system. These techniques are usually applied during acute experiments, and are often limited to recordings from single neurons or fibers, or multiunit recordings from nerve trunks or bundles.

Chronic simultaneous recordings from many neurons and peripheral fibers would lead to a greater understanding of signal transmission in the nervous system. To achieve this goal, several investigators have suggested and studied the use of a sieve electrode array in which a thin diaphragm with many small holes is positioned between the cut ends of a peripheral nerve [4]–[10], [12]; the nerve is left to regenerate through the holes and reinnervate its target organ. Since the positions of the regenerated axons relative to recording/stimulating sites fabricated adjacent to the holes are fixed, long-term recording and stimulation of axons can be successfully achieved. The recordings obtained this way can help to further our understanding of the nervous system and can be used to generate control signals for manipulation of prosthetic devices for amputees and for stimulation of paralyzed muscles [4]–[6]. A thorough review of the history of the development of sieve electrodes has recently been presented by Kovacs *et al.* [4], along with their application to nerve regeneration. The specific application in our case is to use the electrodes for electrophysiological study of the taste-afferent fibers of rats during the controlled stimulation of the tongue. Therefore, there is a need to develop not only sieve-type substrates with a high density of various size through-holes, which allow regeneration of individual axons of varying diameters, but also recording/stimulating sites in proximity to these holes to achieve chronic electrophysiological recordings and stimulations [7].

Various techniques and materials have been used to fabricate the needed sieve electrodes. Some early electrodes were realized by embedding 25-μm-diameter hollow gold cylinders into porous Teflon^{TM} [9]. Others were realized by mechanically drilling 100-μm-diameter holes into epoxy modules, and then embedding $\approx$ 77-μm-diameter Teflon-coated silver wires into the holes [8]. Laser drilling techniques were also used to open through-holes in silicon substrates, producing holes with 50-μm entrance and 25-μm exit diameters; more advanced laser drilling techniques produced 8-μm entrance and exit diameters on 100-μm-thick silicon substrates [10]. Another technique implemented tubular electrode arrays using stacked planar arrays of conductive traces on flexible substrates, resulting in arrays of tubes with 10–15 μm in height, 10–15 μm in width, and 300–1200 μm in length [11]. These techniques had a number of shortcomings: they were generally complex, had to be performed on a single device at a time, lacked the required reproducibility and uniformity, were limited in the minimum size and density of holes that could be reliably formed, and were not compatible with CMOS circuitry.

Semiconductor fabrication techniques, including wet and dry etching of silicon substrates, have also been developed to

Manuscript received March 4, 1992; revised February 8, 1993. This work was supported by the National Institutes of Health under Grant DC00059 to R. M. Bradley. The work of T. Akin was initially supported by the NATO Science Scholarship Program through the Scientific and Technical Research Council of Turkey (TUBITAK).

T. Akin and K. Najafi are with the Center for Integrated Sensors and Circuits, Department of Electrical Engineering and Computer Science, University of Michigan, Ann Arbor, MI 48109 USA.

R. H. Smoke is with the Department of Cardiology, University of Michigan, Ann Arbor, MI 48109 USA.

R. M. Bradley is with the Department of Biologic and Materials Sciences, School of Dentistry, and the Department of Physiology, School of Medicine, University of Michigan, Ann Arbor, MI 48109 USA.

IEEE Log Number 9401227.

0018–9294/94$04.00 © 1994 IEEE

fabricate sieve electrodes [4]–[6], [12]. One early attempt was to fabricate the sieve electrodes by etching arrays of $200 \times 200\,\mu m^2$ through-holes in a ≈200-μm-thick (100)-oriented silicon substrate using a pyrocatechol-based solution [12]; these electrodes also included on-chip buffer transistors which contributed more thermal noise than expected, preventing their successful usage. Later, more successful semiconductor techniques were developed and utilized to fabricate the sieve electrodes. One of them used potassium hydroxide to etch 120 μm × ≈ 1.5 mm slots on (110)-oriented 140-μm-thick silicon substrates, which had ten gold recording sites connected to the external world using Teflon-coated platinum–iridium wires wedge-bounded to the gold bonding pads [6]. Another technique used plasma etching of (100)-oriented silicon wafer, resulting in 8–14-μm-diameter through-holes in 50–100-μm-thick substrates with $\approx 2750\text{-}\mu m^2$ iridium recording sites placed around the holes [4], [5].

These fabrication techniques also have some shortcomings. They are somewhat limited in the minimum achievable hole dimensions (hole diameters are typically larger than 8 μm since they are etched in substrates thicker than 50–100 μm) and the achievable hole densities. The ability to fabricate small hole diameters with high hole densities is a desirable feature to enable one to record from single fibers. Another limitation of some of these techniques is their lack of compatibility with a standard CMOS process [6], [12] that may be needed for some applications where incorporation of on-chip circuitry is critical to the long-term reliability of the implanted system. Many of the presently developed implantable electrodes and systems also suffer from the lack of a reliable lead transfer and connector technology [4]–[6], [12]. The use of lead wires creates mechanical and electrical instability at the bonding points to the electrode [6]. The long-term stability and integrity of any chronically implanted electrode is primarily determined by the stability of the leads that transmit the low-level signals recorded by the high-impedance sites to the outside world.

This paper reports the development of a new micromachined silicon sieve electrode fabricated using silicon micromachining techniques [13] which overcomes the shortcomings of previously reported devices. The fabrication process for the electrode is simple, high-yield, uniform, and reproducible; it can generate a variety of electrode structures, can produce hole sizes as small as 1 μm in diameter, and allows the fabrication of structures with large numbers of holes and hole densities. In addition, the process is compatible with the fabrication of a silicon-based ribbon cable interconnect technology for the reliable transfer of multiple leads to the outside world [14], as well as CMOS circuitry for the fabrication of on-chip electronics. Section II describes the structure and the requirements of a typical sieve electrode. Section III will present the fabrication technology for the implementation of these electrodes and experimental results, and Section IV presents electrical test results for iridium-based recording and stimulating sites. Section V will briefly present a summary of initial *in vivo* test results, which are presented in detail elsewhere [15], and Section VI will provide concluding remarks.

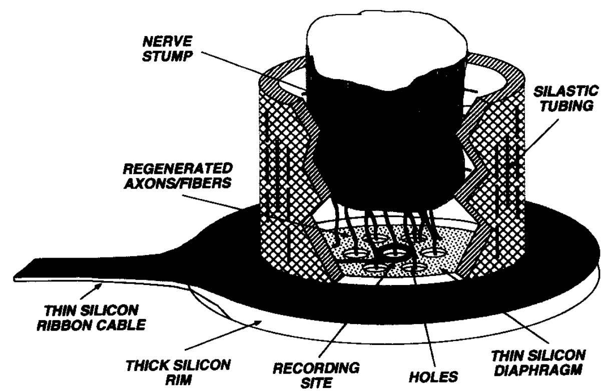

Fig. 1. The overall structure of the sieve electrode along with its application in nerve regeneration.

II. Electrode Structure and Requirements

A suitable sieve electrode and its fabrication technology should meet a number of requirements for most nerve regeneration applications. The fabrication technology should be capable of producing very small holes of various sizes (to allow recordings of individual axons) at high densities with high reproducibility and uniformity. The electrode should be made from biocompatible materials, should be capable of supporting recording and stimulating sites around the holes for close coupling to the axon, should be as thin as possible in order to facilitate nerve regeneration, and should be capable of chronic implantation such that the electrical and physical characteristics of the electrode remain stable. This latter requirement dictates that the recording/stimulating site material have a low and stable interface impedance in extended exposure to biological fluids. We have developed a sieve electrode that satisfies these requirements and that has been successfully used in nerve regeneration applications [13], [15].

The structure of the proposed sieve electrode along with its application in nerve regeneration is shown in Fig. 1. The two ends of a severed nerve are placed inside silastic tubes that are fixed to the two sides of a micromachined silicon substrate. Regeneration occurs between the nerve ends through the holes created in the micromachined silicon substrate. The substrate consists of a thick silicon support rim (≈15 μm thick) and a thin diaphragm (≈4 μm thick). The thin diaphragm supports different size holes and planar thin-film recording/stimulating sites placed around the holes. These implanted electrodes are connected to the outside world using a thin silicon ribbon cable (≈4 μm thick), which is integrated with the electrode and is fabricated at the same time the electrode is formed. It should be noted here that Fig. 1 does not show the actual number of axons, holes, hole-site structures, the other side of the silastic tube, and the other side of the nerve stump.

The above structure provides a suitable environment for successful regeneration of axons through the micromachined holes. The thin diaphragm minimizes the separation between nerve ends, while providing a well-defined region and hole configuration for regeneration; the thick support rim allows for easy handling and mounting. On-chip thin-film recording and

stimulating sites are placed very close to the hole opening, and thus facilitate close coupling to the axon regenerated through the hole. The ability to incorporate an integrated silicon-based cable is desirable for long-term recordings/stimulating applications.

III. Fabrication Process and Results

A summary of the fabrication process is shown in Fig. 2. The process is performed on (100)-oriented silicon wafers having standard thickness and concentration. The wafers are first oxidized, and the oxide is patterned and removed where the thick boron-doped rim regions are to be formed. A deep boron diffusion that defines the 15-μm-thick support rim is performed using a 5-h predeposition at 1175°C followed by a 5-h drive-in at 1200°C. The oxide is removed, and the wafers are oxidized and patterned again for a second boron diffusion. A shallow boron diffusion is performed for 30 min at 1175°C to create a 2.5-μm-thick silicon diaphragm and a silicon base for the fabrication of a multilead ribbon cable. The silicon diaphragm is selectively protected by an oxide mask where holes are to be created. This will allow the fabrication of a number of different-size holes using a single mask without any additional processing steps. It should be noted that thin diaphragms are especially desirable because nerve regeneration can be accelerated when the nerve ends are placed as close to each other as possible. The diaphragm thickness can easily be changed by varying the time and temperature of the shallow boron diffusion, if necessary. After this diffusion, a multilayer bottom dielectric consisting of 3000-Å silicon dioxide, 1500-Å silicon nitride, and 3000-Å silicon dioxide is deposited using low-pressure chemical-vapor deposition (LPCVD). These layer thicknesses are chosen to create a stress-free dielectric film to avoid warping of the substrate and the ribbon cable. Following bottom dielectric deposition, a 9000-Å LPCVD polysilicon is deposited, and doped with phosphorus for 30 min at 950°C to provide a low sheet resistance of $\approx 10\,\Omega$ per square. The doped polysilicon is now patterned using a reactive ion etching (RIE) process (which uses SF_6 and O_2 gases with a ratio of 4:3) to form conductors for recording/stimulating electrodes. The conductors are next insulated with a 2000-Å silicon dioxide layer obtained by wet thermal oxidation, which is followed by the deposition of a second multilayer dielectric film of LPCVD insulating films similar to the bottom dielectric layers. These top dielectric layers are now selectively removed over the sites and bonding pads using an RIE process (which uses CF_4 and CHF_3 gases with a ratio 1:1 for silicon dioxide etching and CF_4 and O_2 gases with a ratio of 40:1 for silicon nitride etching) down to the polysilicon layer. These openings are then inlaid with sputtered 300-Å titanium and 2000-Å iridium films. The extra metal outside the site and bonding pad areas is removed using a life-off technique; therefore, the sites are self-aligned with respect to the polysilicon conductors. The titanium layer is deposited to improve adhesion between polysilicon and iridium. The final step is the removal of the dielectric films in the field regions and in the areas where holes are to be created using an RIE process. The hole diameter is thus defined by the dielectric mask and the anisotropic nature of the RIE etch. This final RIE process is used to etch six layers of dielectrics; therefore, chromium is used as the mask for this etch. The chromium layer is removed after the final RIE using a wet etchant that does not attack the iridium sites. The silicon wafer is next etched in a mixture of ethylenediamine, pyrocatechol, and water (EDP) [2]. Following the EDP etch, the electrodes with the boron-doped silicon substrate become free of the wafer. It should be noted that EDP dissolves only the undoped silicon wafer, but does not attack either silicon that is heavily doped with boron to concentrations greater than $5 \times 10^{19}\ \mathrm{cm}^{-3}$, or any of the other electrode materials. The electrodes are now removed from the etch, rinsed, and ready for bonding and mounting.

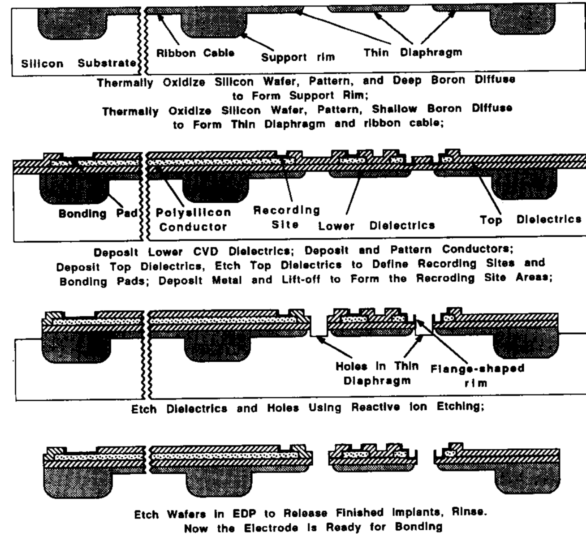

Fig. 2. Summary of the fabrication process of sieve electrodes.

This fabrication process has a number of advantages. It is single-sided, has high yield, requires only five masks, utilizes standard integrated circuit fabrication technologies, is very uniform and reproducible, and is compatible with the fabrication of integrated silicon cables as well as CMOS circuitry [16]. In addition, it is very versatile in that it allows a variety of hole and recording/stimulating site structures to be fabricated without any additional processing steps.

Detailed cross-sectional diagrams illustrating the fabrication of two possible hole-site structures in the same run are shown in Fig. 3. As seen in Fig. 3(a), the hole etched in the dielectric film is surrounded by the polysilicon conductor, which fully supports the iridium site. This hole-site configuration provides a well-defined site surface area and places the recording/stimulating surface close to the hole. The minimum separation between the edge of the polysilicon conductor and the through-hole in this structure is defined by the minimum alignment tolerance required for photolithography. With the current technology at the University of Michigan, it is possible to achieve separations as small as 2 μm (with other technologies, it is possible to decrease the overall size of the hole-site structures and the diameters of the holes even

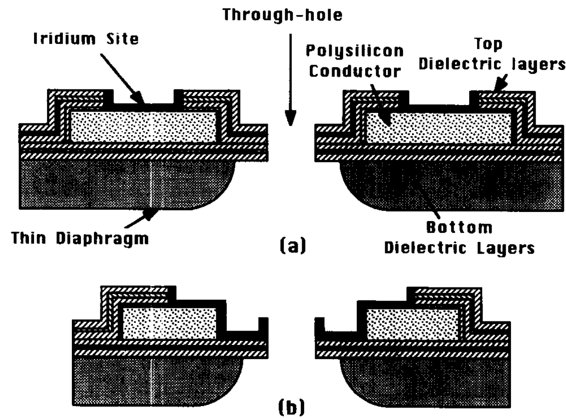

Fig. 3. Detailed cross-sectional diagrams illustrating the fabrication of two possible hole-site structures.

further). It should be noted here that in this fabrication process, the total site area is increased since iridium is deposited on the sidewalls of the sites due to the good step coverage provided by the sputtering process.

If closer placement of the iridium surface to the regenerated axon is required, the hole-site structure shown in Fig. 3(b) can be used. In this structure, the iridium layer overlaps the polysilicon conductor, where contact is to be achieved, and is extended over the field dielectrics to the edge of the hole. The hole is created in the dielectric film by using the iridium site as a masking layer during the RIE etching process, thus making it self-aligned with respect to the edge of the iridium site. It should be noted that iridium sites are not etched during the final RIE process. The advantages of this second structure are that the recording/stimulating sites are closer to the holes, and that flange-shaped iridium rings are formed around the holes. These rings are formed during the last two masking steps in the process. In the third masking step (which involves the patterning of photoresist in the shape of the sites and bonding pads, etching of the top dielectrics using RIE, and deposition and liftoff of the iridium), photoresist is maintained over the field dielectrics where the holes are to be formed. Sputtered iridium has a very good step coverage and coats the sidewalls of this photoresist and the sidewalls of the underlying dielectrics. When the photoresist is removed during the liftoff process, the iridium on the sidewalls of the photoresist remains. After patterning the final dielectric mask, the dielectrics where the holes are to be created are etched using the final RIE process. This final RIE step etches through the entire thickness of the top and bottom dielectrics and reaches the substrate. It is during this last RIE step that the iridium acts as a mask against RIE and allows the exposed dielectrics to be etched to create a hole that is self-aligned with respect to the iridium sites. It should be noted that this RIE step does not etch the iridium which has been coated on the sidewalls of the dielectrics. Consequently, with the removal of these dielectrics, the iridium that has been coated on the sidewalls of the previous photoresist and the sidewalls of the dielectrics remains, thus creating the hole-site structure with flange-shaped rings. One can expect that this hole-site structure will provide maximum coupling between the regenerated axon and the recording/stimulating surface, thus improving the overall signal-to-noise ratio of recorded signals and decreasing the maximum current necessary for stimulation. In addition, this second structure almost doubles the density of holes because of the smaller required area for the site.

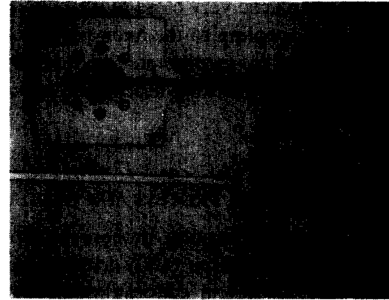

Fig. 4. Optical photograph of two sieve electrodes with integrated silicon ribbon cables.

Fig. 5. An SEM view of the thin diaphragm of one of the sieve electrodes.

Fig. 4 shows optical photographs of the front and back sides of two fabricated sieve electrodes with integrated silicon ribbon cables. Fig. 5 shows a scanning electron microscope (SEM) view of the thin diaphragm of one of them. Notice that the diaphragm is surrounded by 100-μm -diameter holes to allow adhesives to get through during the process of the attachment of the silastic tubes to the silicon support rim. The sieve electrode is 1×1 mm and the thin diaphragm has a diameter of 400 μm. The silicon ribbon cable has a thickness of 4 μm, a width of 60 μm, a length of ≈ 2.4 cm, and carries five 5-μm-wide polysilicon conductors that interconnect the recording sites with bonding pads.

Fig. 6 shows close-up SEM views of the first and second hole-site structures with site areas of about 100 μm^2, where the hole diameters are about 2 and 5 μm, respectively. Fig. 7 shows the SEM view of the cross section of the first hole-site structure. Several observations should be made with respect to these figures. First, in the first structure, the hole size is defined either by dielectric openings during the final RIE, or by the selectively protected areas of the silicon substrate during the shallow boron diffusion. Second, the silicon substrate can be removed completely, if required, since the dielectric layers (that are approximately 1.4 μm in total thickness) are

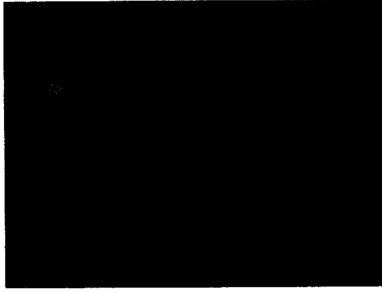

Fig. 6. Close-up SEM views of the first and second hole-site structures with site areas of about 100 μm^2, where the hole diameters are about 2 and 5 μm, respectively.

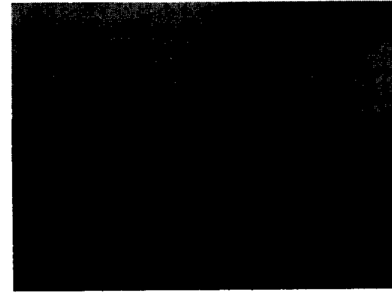

Fig. 7. The cross section of the first hole-site structure.

Fig. 8. SEM view of a 1-μm flange-shape side obtained in the second hole-site structure.

Fig. 9. SEM view of a complete sieve electrode with the second hole-site structure.

sufficiently strong to form the diaphragm. Third, in the second structure, the hole diameter is defined by the iridium site; thus, the site is next to and self-aligned to the hole. Fourth, due to good step coverage of the sputtered iridium film, the iridium is deposited on the sidewalls of the dielectric, thus creating a flange-shaped ring in the second structure. This structure results in a total effective surface area that is larger than that without the extra lip, without increasing the geometric area of the site, and improves coupling between the site and the regenerated axon. Fifth, since the iridium is supported on the bottom dielectrics, it is very strong and does not break off during any of the fabrication steps. Fig. 8 shows an SEM view of a 1-μm-diameter flange-shaped site. Sites like this can be reproducibly and reliably formed. Fig. 9 shows an SEM view of a complete sieve electrode with the second hole-site structure, where it can be seen that none of the fabricated sites is damaged. We have obtained better than 90% yield (based on optical inspections of the sites and sieve electrodes) with these structures.

Because of the flexibility allowed by the fabrication process in reducing the total hole-site area and hole diameters, many different sieve electrode designs can be fabricated in a single fabrication run on the same mask. A number of sieve electrodes with a variety of hole sizes and configurations were fabricated using the above process; a list of the designs is shown in Table I. Designs include sieve electrodes with hole diameters as small as 2 μm and center-to-center spacing as small as 10 μm. Electrode designs 1–6 utilize the first hole-site structure, while the rest utilize the second hole-site structure. The ability to set hole diameters, site areas, and hole density as required is a desirable feature for nerve regeneration applications. Some applications require a large number of small diameter holes in a fairly small area, while others require larger hole sizes in a rather large area. In addition, different types of openings on the diaphragm can be formed for some other applications; Fig. 10 shows a diaphragm with 2-μm grooves. We believe that the above process satisfies the requirements for most applications.

IV. Electrical Characteristics

The electrical characteristics of any recordings/stimulating electrode are very crucial for its succesful interface to the tissue. For recording applications, it is desirable to obtain sites

TABLE I
A SUMMARY OF FEATURES AND CHARACTERISTICS OF VARIOUS SIEVE ELECTRODE DESIGNS

Design No.	No. of 2-μm-Diam. Holes	No. of 5-μm-Diam. Holes	No. of 10-μm-Diam. Holes	No. of 15-μm-Diam. Holes	No. of Hole-Site Structures
1	151	—	—	—	151
2	777	—	—	—	5
3	—	497	—	—	5
4	540	1	—	52	5
5	197	—	—	133	5
6	—	174	—	133	5
7	286	—	—	—	286
8	—	214	—	—	214
9	—	—	132	—	132
10	5	130	170	—	05

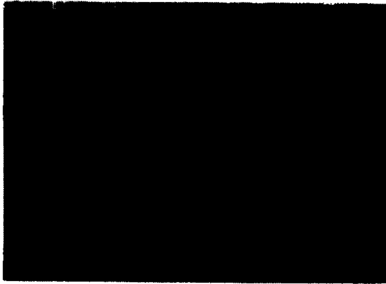

Fig. 10. The diaphragm of a sieve electrode with 2-μm grooves.

that have a small area and as small an electrode–electrolyte interface impedance as possible in order to maximize the signal-to-noise ratio. For stimulating electrodes, it is desirable to achieve maximum charge delivery capacity in a small area, so that precise charge packets can be delivered to the axon under investigation without creating any stimulating artifacts in the adjacent axons. The requirements of both recording and stimulating applications can be satisfied by using anodized iridium oxide (AIROF) as the electrode site material [17], [18] in these sieve electrodes.

We have fabricated a variety of electrodes having iridium sites of varying area. After their final etching and release from the host wafer, the electrodes are mounted and bonded for electrical testing. The iridium sites are first tested to measure their impedance before activation. They are then activated in a phosphate-buffered saline solution using cyclic voltammetry. The activation (i.e., growth of a layer of anodized iridium oxide film, AIROF) is achieved by cycling the iridium sites between potential levels of -0.9 and 1.1 V with respect to an SCE reference electrode using a triangular voltage ramp at 2.1 V/s [17]. After about 50 min of activation, the electrode charge storage capacity [18] and electrode–electrolyte impedance are measured. In order to determine the charge delivery capacity of the AIROF sites, they are subjected to cathodic-first, charge-balanced, biphasic, constant current pulses of

TABLE II
SUMMARY OF SITE IMPEDANCES AND CHARGE DELIVERY CAPACITIES FOR ACTIVATED IRIDIUM OXIDE ELECTRODES

Site Area (μm^2)	Impedence @ 1 kHz Before Activation (MΩ)	After Activation (kΩ)	Charge Storage Capacity (mC/cm^2)	Charge Delivery Capacity (mC/cm^2)	Maximum Stimulation Current (μA)
42	2.80	186.7	57.3	5.7	12
68	2.18	150.3	83.3	5.3	18
101	1.62	102.2	77.2	4.8	24
127	1.48	89.9	92.7	4.6	32
186	1.03	74.9	37.7	4.1	38

varying amplitude until the onset of gas evolution (which is detected when the voltage drop across the electrode–electrolyte interface exceeds the water window, which was assumed to be -0.9 V versus SCE in our measurements) is reached. These maximum current levels together with the duration of the current pulse (which has been fixed at 200 μs for our electrodes) provide a measure of the maximum deliverable charge into the tissue through the AIROF sites.

Electrical test results on a number of fabricated sites are summarized in Table II. The site areas range from 42 to 186 μm^2 and exhibit impedances ranging from 2.8 to 1.0 MΩ at 1 kHz before activation. Once activated, the site impedances reduce to 187–75 kΩ at 1 kHz due to the growth of the iridium oxide film. The total charge storage capacity of the sites varies from site to site and is indicated in Table II for each site. These activated sites provide a high charge delivery capacity approaching of 6 mC/cm^2. Notice that the charge delivery capacity is dependent on the site area. The maximum injected current levels for these electrodes increase with site area, as expected, and vary between 10 and 40 μA.

Several observations should be made with respect to the above results. First, the site impedances after activation are very low and provide an appropriate interface between the electrode and the neural signal traveling through the axon. Our colleagues at the University of Michigan have used similar electrodes for recording single-unit discharges from cortical neurons and have obtained high-quality signals for periods of more than a few months [19], and have demonstrated the biocompatibility of the materials used in these sieve electrodes [20]. We have not observed any gross charges in the impedance of the unactivated iridium sites after keeping them in the animals for more than three months. Second, the charge delivery capacity together with the maximum deliverable current exhibited by these electrodes should be sufficient for successful stimulation of neural structures. Experience with similar electrode surfaces has shown that the threshold current for many neural structures is typically between 1–10 μA [21]. We expect that these sieve electrodes will require similar, possibly even smaller, current levels to stimulate individual axons since the stimulating surfaces are very close to the axon. If higher levels of stimulating currents are needed, either the site area can be increased or the simulation protocol can be modified through appropriate biasing of the electrode [22].

Third, the above electrical characteristics are achieved in an area of less than a few hundred square microns, thus allowing a large number of sites to be positioned in a small area. This is a desirable feature in both electrophysiological studies and in the development of closed-loop prostheses where direct connection to a large number of axons is required.

Another important consideration with regard to the electrical characteristic of the electrode is its contribution to the total noise of the recording system. The two primary components of noise are electrode noise and biological noise. The main source of electrode noise is thermal noise, which is proportional to the real part of the electrode–electrolyte impedance [24]. This thermal noise has a $1/f$ frequency dependence, similar to the electrode impedance. Therefore, the total contribution of this noise is determined by the recording bandwidth, as well as the electrode impedance. The total noise voltage of a 100-μm^2 iridium electrode site has been measured to be 7.3 μV rms over a 100-Hz–15-kHz bandwidth. This is similar to the measured noise voltage of gold recording sites, as expected since the interface impedance of most metal electrodes is dominated by the double layer formed at the electrode–electrolyte interface. Our experience with gold recording sites has also shown that the electrode thermal noise is small when compared to biological noise. More information on the noise contribution of metal electrodes can be found in [11], [23].

V. *In Vivo* Experiments and Results

To evaluate the potential of these sieve electrodes in nerve regeneration applications, we implanted them between the cut ends of the rate glossopharyngeal nerve (IX cranial nerve) which innervates taste and somatosensroy receptors on the posterior tongue. Sieve electrodes were implanted in rats for times range from 91 to 118 days, after which the regeneration was evaluated. Based on gross examination of the implants the histological examination of the nerve cross sections distal to the sieve electrode, regeneration through the electrode occurred in 21 of the 28 implants [15]. When regeneration was successful, the glossopharyngeal nerve was clearly visible in the guide tubes, and numerous myelinated fibers were present in the cross section of the nerve distal to the sieve electrode [15]. In addition, the functionality of the regenerated nerves was tested by first cutting the nerve from the side central to the sieve electrode, and then connecting a pair of platinum–iridium hook electrodes between the cut end of the nerve bundle close to the sieve electrode and a nearby tissue for reference. The neural activity from the whole nerve was analyzed by passing it through an integrator (with a time constant of 0.5 s) connected to a pen recorder, while the nerves' receptive fields in the oral cavity were stimulated with chemical, mechanical, and thermal stimuli. Responses were obtained to all these stimuli, indicating that the glossopharyngeal nerve had regenerated and formed functional connection with receptors, as seen in Fig. 11. It should be noted here that these recordings are not spontaneous action potentials, but rather whole nerve recordings, consisting of asynchronously occurring compound action potentials which are rectified and smoothed to give a dc signal. These responses were similar to whole nerve recordings

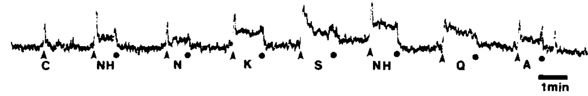

Fig. 11. Integrated recordings (time constant = 0.5 s) of whole nerve responses from a glossopharyngeal nerve that had regenerated through a sieve electrode. Arrowhead indicates time of stimulus applications and dots distilled water rinses applied to the posterior tongue. C = ice cold water thermal stimulus, $NH = 1.0M$ NH_4Cl, $N = 1.0$M NaCl, $K = 1.0$M KCl, $S = 1.0$M NaSaccharin, $Q = 0.01$M quinine HCl, $A = 0.1$M citric acid.

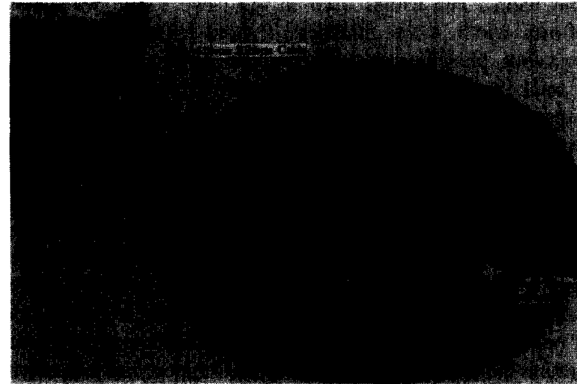

Fig. 12. A complete structure of passive sieve electrodes for a chronic setup for long-term recordings. The picture shows the silastic tubes attached to a separate electrode without a cable.

from an intact glossopharyngeal nerve, confirming the good quality of the regenerations. Comparisons of recordings and the number of regenerated taste buds between operated and unoperated intact glossopharyngeal nerves can be found in [15], which also includes more information on the experimental procedure.

We have also implanted a number of sieve electrodes with various hole sizes, and configurations have been implanted to determine the optimum electrode structure, hole sizes, and hole densities. We have not observed any systematic difference in the extent of the regeneration with the use of different hole configurations of the sieve designs [15]. Currently, we have chronically implanted more sieve electrodes to obtain long-term recordings from multiple axons using the sites on the electrodes. Many of these electrodes including integrated silicon ribbon cables which will allow long-term recordings to be made from five sites. Fig. 12 shows a sieve electrode prepared for long-term recording, which consists of the electrode with the ribbon cable, silastic tubes attached to the electrode, and the external connector. The picture shows the silastic tubes attached to a separate electrode instead of the one connected to the connector through the silicon ribbon cable in order to clearly show the electrode, tubes, the silicon ribbon cable, and the connector.

The mechanical strength of the electrodes and the ribbon cable and their resistance to breakage during handling have been a main concern in chronic experiments. Our experiments have shown that although these electrodes are very thin, they are not fragile; none of them was broken during the implantations. In addition, none of the thin diaphragms was

damaged during the silastic tube attachment or after the implantations since, after silastic tubes are attached, there is no force on the thin diaphragms. However, special handling is necessary while implanting the electrodes with cables, as dictated by the particular surgical procedure and the anatomy of the implant site.

The ability to integrate the ribbon cable with the electrode is a major advantage in chronic applications. The silicon ribbon cable is strong, yet very flexible [14]. The flexibility and strength of the cable can be adjusted by changing its thickness and width. The cables used in the sieve electrodes have a 60-μm width, 4-μm thickness, 2.4-cm length, and carry 5-μm-wide phosphorous-doped polysilicon leads, each having a total series resistance of about 50 kΩ and a total shunt capacitance of 5.6 pF to the substrate and to the tissue (which is assumed to be at ground for all practical purposes). If a smaller interconnect resistance is needed (which may be necessary for stimulation applications), the polysilicon conductors can be replaced by tantalum or other refractory metals. Because of the long length of the cable, special handling and some means of protection to decrease the direct pressure on the cable might be necessary when the cable is to be placed near a muscle. In such applications, silastic tubes can be placed around the cable to provide additional support and prevent the application of direct pressure on it. It should be mentioned here that the use of integrated silicon ribbon cable simplifies the bonding to the electrode since bonding takes place between the connector and the pads on the ribbon cable directly, far away from the electrode. In addition, the bonding areas can easily be insulated to obtain a more reliable system for chronic recording experiments. Chronic recording experiments aimed at obtaining long-term recordings from these electrodes are presently underway.

Long-term recording and stimulation using these five-channel passive electrodes will provide us with improved understanding of the operation of the test system. It is believed, however, that in order to gain insight into the complex organization of the peripheral nervous system, recording and stimulation of a large number of axons may be required. In order to achieve this goal, circuitry that can scan a large number of sites and can transmit the recorded data to the outside world chronically should be included on the electrode. Therefore, active sieve electrodes with on-chip circuitry are being developed for these applications. This circuitry includes a selector that can be programmed by the user to record activity from a number of sites, per-channel amplifiers to amplify the recorded signals, and an analog mutliplexer. The entire proposed system interfaces with the outside world through an inductively coupled bidirectional RF telemetry link which is used to transmit power, channel selection data, and recorded data between the implant and an external transmitter. This system approach could also be used as the neural interface to a prosthetic device and for simulation applications.

VI. Conclusions

We have developed and fabricated a micromachined silicon sieve electrode to record and stimulate individual axons of the peripheral-nerve system by utilizing the nerve regeneration principle. The fabrication process utilizes deep and shallow boron diffusions together with reactive ion etching to fabricate holes of varying diameters. These holes are surrounded by anodized iridium oxide recording/stimulating electrodes, which allow long-term recording and stimulation of individual regenerated axons. These sites are connected to the outside world using integrated silicon ribbon cables. A number of sieve electrodes with hole diameters as small as 1 μm and site impedances of less than 100 kΩ @ 1 kHz are fabricated using the above fabrication technology. These sites can also be used for the stimulation of axons and to provide charge delivery capacities approaching 6 $\mathrm{mC/cm^2}$. thus allowing the stimulating current pulses of up to 40 μA with 200- μs pulse widths to be injected into the tissue. The sieve electrodes were implanted between the cut ends of peripheral taste fibers of rates (glossopharyngeal nerve), and have successfully regenerated through the holes, based on the gross examination of the implants and histological examination of the nerve cross section distal to the electrode. In addition, electrophysiological recordings from the central end of the regenerated nerve obtained by external electrodes show that these regenerated taste buds are functional and respond to chemical, mechanical, and thermal stimulation of the tongue.

Acknowledgment

The authors would like to thank T. Hull in assisting in the fabrication of the electrodes.

References

[1] M. Salcman and M. J. Bak, "Design, fabrication, and in-vivo behavior of chronic recording intracortical microelectrodes," *IEEE Trans. Biomed. Eng.*, vol. BME-20, pp. 253–260, July 1973.

[2] K. Najafi, K. D. Wise, and T. Mochizuki, "A high-yield IC-compatible multichannel recording array," *IEEE Trans. Electron Devices*, vol. 32, pp. 1206–1211, July 1985.

[3] R. D. Purves, *Microelectrode Methods for Intracellular Recording and Ionophoresis*. London: Academic, 1981, pp. 1–146.

[4] G. T. A. Kovacs, C. W. Stormet, and J. M. Rosen, "Regeneration microelectrode array for peripheral nerve recording and stimulation," *IEEE Trans. Biomed. Eng.*, vol. 39, pp. 893–902, Sept. 1992.

[5] G. T. Kovacs, "Regeneration microelectrode arrays for direct interface to nerves," in *Tech. Dig. 6th Int. Conf. Solid-State Sensors and Actuators (Transducers '91)*, San Francisco, CA, June 1991, pp. 116–119.

[6] D. J. Edell, "A peripheral nerve information transducer for amputees: Long-term multichannel recordings from rabbit peripheral nerves," *IEEE Trans. Biomed. Eng.*, vol. BME-33, pp. 203–214, 1986.

[7] R. Llinas, C. Nicholson, and K. Johnson, "Implantable monolithic wafer recording electrodes for neurophysiology," in *Brain Unit Activity During Behavior*, M. Phillips, Ed. Springfield, IL: Thomas, 1973, ch. 7, pp. 105–111.

[8] A. Mannard, R. B. Stein, and D. Charles, "Regeneration electrode units: Implants for recording from peripheral nerve fibers in freely moving animals," *Science*, vol. 183, pp. 547–549, 1974.

[9] A. F. Marks, "Bullfrog nerve regeneration into porous implants," *Anatomical Rec.*, vol. 163, p. 266, 1969.

[10] J. M. Rosen, G. T. A. Kovacs, M. Stephanides, D. Marshall, M. Grosserm, and V. R. Hentz, "The development of a microelectronic axon processor silicon chip neuroprosthesis," in *Proc. 10th Int. Conf. Ass. Adv. Rehab. Tech.*, San Jose, CA, June 1987, pp. 675–677.

[11] G. E. Leob, W. B. Marks and P. G. Beatty, "Analysis and microelectronic design of tubular electrode arrays intended for chronic, multiple single-unit recording from captured nerve fibers," *Med. Biol. Eng. Comput.*, vol. 15, pp. 195–201, Mar. 1977.

[12] T. Matsuo, A. Yamaguchi, and M. Esashi, "Fabrication of multi-hole-active electrode for nerve bundle," *J. Japan Soc. ME & BE*, July 1978.

[13] T. Akin and K. Najafi, "A micromachined silicon sieve electrode for nerve regeneration applications," in *Tech. Dig. 6th Int. Conf. Solid-State Sensors and Actuators (Transducers '91)*, San Francisco, CA, June 1991, pp. 128–131.
[14] J. F. Hetke, K. Najafi, and K. D. Wise, "Flexible silicon interconnects for microelectromechanical systems," in *Tech. Dig., 6th Int. Conf. Solid-State Sensors and Actuators (Transducers '91)*, San Francisco, CA, June 1991, pp. 764–767.
[15] R. M. Bradley, R. H. Smoke, T. Akin, and K. Najafi, "Functional regeneration of glossopharyngeal nerve through micromachined sieve electrode arrays," *Brain Res.*, vol. 594, p. 84–90, 1992.
[16] J. Ji and K. D. Wise, "An implantable CMOS circuit interface for multiplexed microelectrode recording arrays," *IEEE J. Solid-State Circuits*, vol. 27, pp. 433–443, Mar. 1992.
[17] D. J. Anderson, K. Najafi, S. J. Tanghe, D. A. Evans, K. L. Levy, J. F. Hetke, X. Xiu, J. J. Zappia, and K. D. Wise, "Batch-fabricated thin-film electrodes for stimulation of the central auditory system," *IEEE Trans. Biomed. Eng.*, vol. 36, pp. 693–704, July 1989.
[18] L. S. Robblee, J. L. Lefko, and S. B. Brummer, "Activated Ir: An electrode for reversible charge injection in saline solution," *J. Electrochem. Soc.*, vol. 130, pp. 731–733, Mar. 1983.
[19] K. D. Wise, Quarterly Progress Rep. 4–6, 1991–1992, on Contract "Multichannel multiplexed intracortical recording arrays," Neural Prosthesis Program, Nat. Inst. for Neurological Disorders and Stroke, Nat. Inst. Health.
[20] J. K. Niparko, R. A. Altschuler, X. Xue, J. A. Wiler, and D. J. Anderson, "Surgical implantation and biocompatibility of CNS auditory prostheses, *Ann. Otol. Rhinol. Laryngol.*, vol. 98, pp. 965–970, 1989.
[21] J. K. Niparko, R. A. Altschuler, D. A. Evans, X. Xue, J. Farraye, and D. J. Anderson, "Auditory brainstem prosthesis: Biocompatibility of stimulation," *Otolaryngol. Head Neck Sug.*, vol. 101, pp. 344–352, 1989.
[22] X. Beebe and T. L. Rose, "Charge injection limits of activated iridium oxide electrodes with 0.2 ms pulses in bicarbonate buffered saline," *IEEE Trans. Biomed. Eng.*, vol. 35, pp. 494–495, June 1988.
[23] D. J. Edell, L. D. Clark, and V. M. McNeil, "Optimization of electrode structure for chronic transduction of electrical neural signals," in *Proc. IEEE EMBS 9th Int. Conf.*. 1986, pp. 1626–1629.
[24] R. G. Gesteland, B. Howland, J. Y. Lettvin, and W. H. Pitts, "Comments on microelectrodes," *Proc. IRE*, pp. 1856–1862, Nov. 1959.

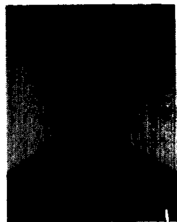

Tayfun Akin (S'90) was born in Van, Turkey, in 1966. He received the B.S. degree in electrical engineering with high honors from Middle East Technical University, Ankara, in 1987 and the M.S. degree in electrical engineering from the University of Michigan, Ann Arbor, in 1989. He is currently a Ph.D. candidate in electrical engineering at the University of Michigan, Ann Arbor.

His research interests include analog and digital intregrated circuit design, silicon-based integrated sensors and tranducers, and implantable microtelemetry systems and transducers for biomedical applications.

Khalil Najafi (S'84–M'86) was born in 1958. He received the B.S.E.E. degree in 1980 and the M.S.E.E. degree in 1981, both from the University of Michigan, Ann Arbor, and the Ph.D. degree in electrical engineering from the University of Michigan in 1986.

From 1986 to 1988 he was employed as a Research Fellow, from 1988 to 1990 as an Assistant Research Scientist, from 1990 to 1993 as an Assistant Professor, and since September 1993 as an Associate Professor in the Department of Electrical Engineering and Computer Science, University of Michigan. His research interests include the development, design, fabrication, and testing of solid-state integrated sensors and microactuators, analog and digital integrated circuits, implantable microtelemetry systems and transducers for biomedical applications, technologies and structures for microelectromechanical systems and microstructures, and packaging techniques for implantable transducers.

Dr. Najafi was the recipient of the Beatrice Winner Award for Editorial Excellence at the 1986 International Solid-State Circuits Conference, and of the Paul Rappaport Award for coauthoring the Best Paper published in the IEEE TRANSACTIONS ON ELECTRON DEVICES. He is an Associate Editor for the *Journal of Micromechanics and Microengineering*.

Richard H. Smoke received to the B.S. degree in physiology from Eastern Michigan University in 1990.

From 1985–1990 he served in the United States Air Force as a Medical Service Specialist. He worked as a Research Assistant in the Department of Biologic and Materials Sciences in the Dental School at the University of Michigan. He is currently with the Department of Cardiology at the University of Michigan.

Robert M. Bradley received the dental degree from the University of London in 1963, the Master's degree in periodontics from the University of Washington in 1966, and the Ph.D. degree in biological sciences from Florida State University in 1970.

His postdoctoral training was completed with Dr. Geoffrey Dawes at the Nuffield Institute for Medical Research at Oxford. He joined the faculty of the University of Michigan in 1972.

In 1990 Dr. Bradley received the Claude Pepper Award of Excellence for his research in the physiology of taste from the National Institutes of Health.